nature sustainability

Article

https://doi.org/10.1038/s41893-022-01037-w

Qatar Peninsula's vulnerability to oil spills and its implications for the global gas supply

Received: 26 May 2022

Accepted: 29 November 2022

Published online: 12 January 2023

Check for updates

Thomas Anselain[1], Essam Heggy[2,3,4] ✉, Thomas Dobbelaere[1] & Emmanuel Hanert[1,5] ✉

More than 20% of global liquefied natural gas (LNG) exports and almost all of Qatar's drinking water production originate from three industrial sites on Qatar's eastern coast. They are all vulnerable to oil spills, and this vulnerability remains largely unquantified. Here we model oil-spill dispersal in the shallow maritime waters surrounding Qatar to identify which offshore areas and times of the year pose the greatest threat to the nation's LNG export and seawater desalination facilities. By combining oil transport simulations with marine traffic data, we identify two high-risk areas, sizing up to ~15% of Qatar's maritime exclusive economic zone. Ras Laffan's LNG terminal has the highest vulnerability to oil spills all year, and its desalination plant, producing 30% of the national water supply, has a seasonal vulnerability peaking to an alarming level twice a year during spring and fall. Both LNG export and desalination facilities could be impacted by oil spills occurring outside of Qatar's maritime borders in less than three days. We suggest that offshore high-risk areas be closely monitored with airborne and satellite synthetic-aperture radar providing early warning for oil spills that could severely disrupt Qatar's LNG exports, further aggravating the global gas crisis.

Qatar is the world's largest producer and exporter of liquefied natural gas (LNG; on par with Australia[1]) and the world's most at-risk country for water scarcity[2]. Located on the eastern side of the Arabian Peninsula, it experiences one of the aridest and most corrosive environments on Earth and has minimal groundwater reserves. Groundwater levels have dropped by several metres since the 1980s because of intensive agricultural use[3]. The primary freshwater aquifer in the north of the peninsula is already severely threatened by seawater intrusion and is hardly usable for human consumption[4]. However, despite this extreme water scarcity, Qatar is also one of the world's wealthiest countries in terms of gross domestic product per capita. This is due to its natural gas reserves, which are the third largest in the world. Most of its gas production is liquefied and exported from the industrial port of Ras Laffan, situated along the northeastern coast.

The hydrocarbon export revenues allowed Qatar to invest heavily in seawater desalination plants to preserve its population from severe water shortages[5]. As a result, Qatar's drinking water now comes almost exclusively from desalination[6], which increased fivefold between 2003 and 2018[4]. Desalination capacity is located mainly in three industrial areas along the eastern coast: Ras Laffan, Ras Abu Fontas and Umm Al Houl (Fig. 1). In 2021, their combined desalination capacity reached about 536 million imperial gallons per day and is expected to reach 636 million imperial gallons per day in 2023[7]. Umm Al Houl produced about 37% of all desalinated water, Ras Abu Fontas 33% and Ras Laffan 30%[7,8].

In 2021, Qatar exported 106.8 billion cubic metres (b.c.m.) of LNG, corresponding to 10.5% of all gas exports and 20.8% of global LNG exports[9]. Qatar LNG export capacities are forecast to increase

[1]Earth and Life Institute, UCLouvain, Louvain-la-Neuve, Belgium. [2]Viterbi School of Engineering, University of Southern California, Los Angeles, CA, USA. [3]Jet Propulsion Laboratory, California Institute of Technology, Pasadena, CA, USA. [4]Qatar Environment and Energy Research Institute, Hamad Bin Khalifa University, Doha, Qatar. [5]Institute of Mechanics, Materials and Civil Engineering, UCLouvain, Louvain-la-Neuve, Belgium. ✉e-mail: eheggy@hbku.edu.qa; emmanuel.hanert@uclouvain.be

https://doi.org/10.1038/s41893-022-01037-w

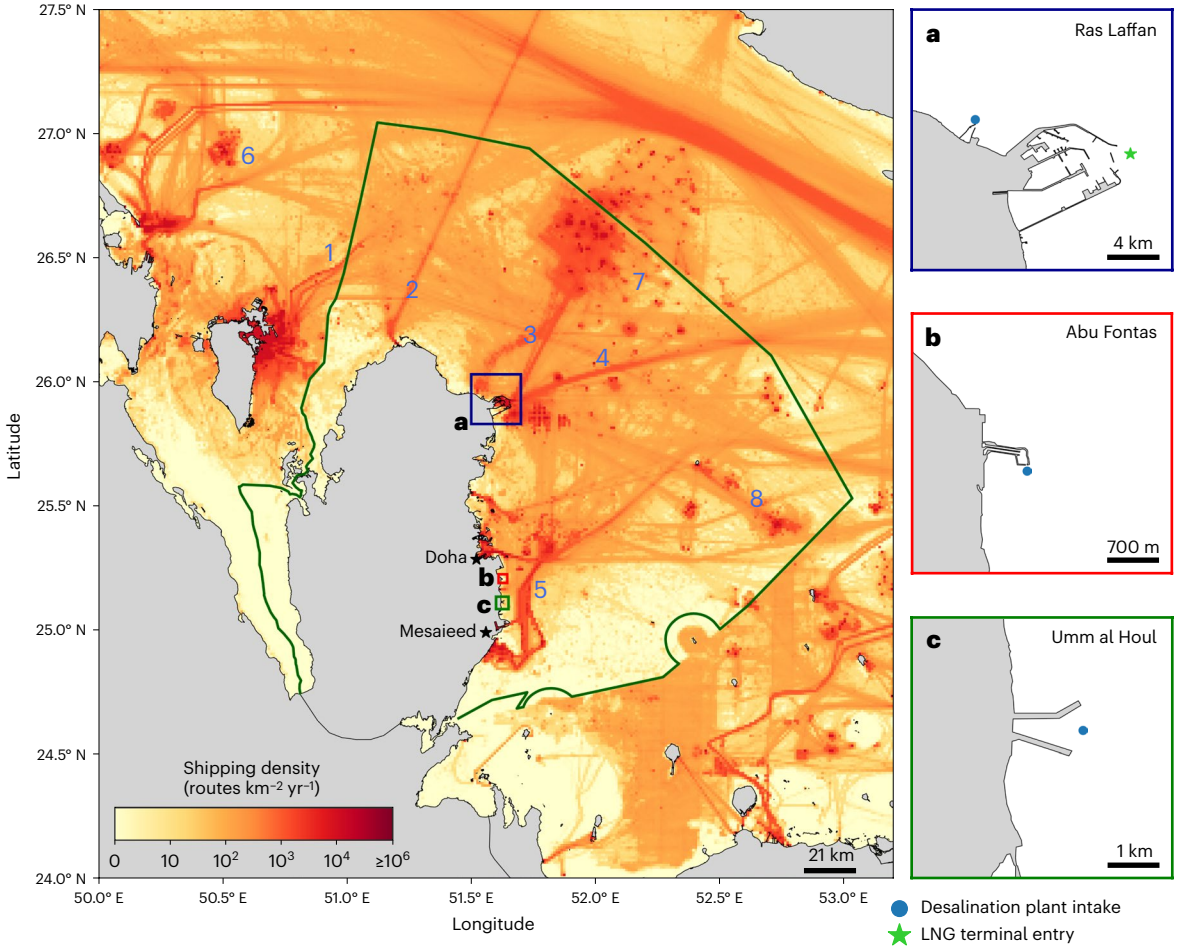

Fig. 1 | Shipping traffic density around Qatar in 2019 with close-up views of the desalination and LNG export infrastructures. Some areas within or close to Qatar EEZ (shown in dark green) have a particularly high shipping density: 1. main shipping route to Bahrain; 2. main shipping route from Qatar to Iran; 3. route from Ras Laffan to Qatar's North Field; 4. main route followed by LNG carriers to/from Ras Laffan; 5. shipping routes to/from the industrial area south of Mesaieed. The shipping density map also highlights the locations of some major oilfields and gas fields close to Qatar: 6. Abu Safah oilfield (KSA), 7. North Field, 8. Bul Hanine and Maydan Mahzam oilfields, and Halul Island terminals. **a**–**c**, Enlargements of areas marked on map: Ras Laffan (**a**), Abu Fontas (**b**) and Umm al Houl (**c**).

to ~151 b.c.m. in 2025 and ~174 b.c.m. in 2027 after the expansion of Ras Laffan's liquefaction units[10]. Currently, natural gas accounts for about a quarter of the global energy mix[9]. The demand for natural gas is expected to continue its growth until about the mid-2030s[11] as it results in less CO_2 emissions compared with oil and coal and is hence considered as a more environmentally friendly option among fossil fuels in the transition towards net-zero emissions by 2050. The global gas market currently has minimal spare capacity as the invasion of Ukraine by the Russian Federation and the sabotaging of the Nord Stream gas pipelines resulted in a substantial reduction in Russian gas deliveries to Europe, which amounted to about 150 b.c.m. in 2021 (corresponding to about 37.4% of all European gas imports). To disengage from Russian gas, Europe is considering importing more LNG. While no single country has the capacity to fully replace the Russian gas supplies, Qatar is nonetheless considered as a key supplier that could partially fill the existing deficit in the upcoming years. Unlike the other two major LNG exporters (Australia and the United States), which have several gas liquefaction facilities spread along their extended coastlines, all of Qatar's LNG production is concentrated in the industrial port of Ras Laffan, whose entrance for tankers is less than 2 km wide.

Pollution from oil spills can severely disturb desalination plants by compromising seawater intake[12] and port activities[13,14] by impeding the passage of vessels during the time oil containment measures (such as booms) are in place. Such disruptions are aggravated in shallow waters where circulation currents are faster and navigation is carried out through narrow dredged maritime canals. With about half of the world's oil reserves[15], the Persian/Arabian Gulf (the Gulf) is one of the most oil-polluted environments in the world. It is a major passage for ships, in particular oil tankers, with about 20,000–30,000 tanker movements per year[16]. Ships themselves are an important source of oil spills through their operational discharges such as tank washings, ballast water discharges and discharges of ship waste containing oil products and through unintentional discharges following sabotaging or accidents. In addition, the Gulf includes 34 major oilfields that are exploited by about 800 wells and 40 major oil terminals[17,18]. On average, 100,000–160,000 tons of oil and its derivative products are accidentally or intentionally released in the Gulf annually. This level of seawater oil pollution is 47 times larger than the world's average pollution level[16].

Qatar is at the crossroads of several maritime transport lines and is thus particularly exposed to oil pollution risks, which could compromise both its desalinated water production and a fifth of the global LNG supply. To mitigate this alarming vulnerability, the early detection of marine pollution is crucial to contain and disperse it before it can reach vital coastal infrastructure. While orbital synthetic-aperture radar (SAR) images provide subsequent monitoring of oil spills[19], the current repeat acquisition time of most SAR satellites in the Gulf

area ranges from three to eight days at best, which compromises the efficiency of tracking oil spills in the nearshore zone. The performance of oil-spill early warning systems can be markedly improved by pre-identifying specific high-risk areas to mitigate the limitations associated with the low-repeat passes. These high-risk areas can then be continuously monitored by combining both airborne and multiple satellite SAR scenes to provide high acquisition frequencies of 12 to 24 h that are needed to mitigate potential major oil spills in Qatar's nearshore zone.

In this Article, we identify where airborne and satellite monitoring resources should be prioritized by computing the oil-spill risk and shipping pollution exposure spatial distributions for the LNG export terminal of Ras Laffan and the desalination plants of Umm Al Houl, Ras Abu Fontas and Ras Laffan (Fig. 1). These infrastructures will be referred to as Qatar's vital coastal infrastructures (QVCIs). We simulate oil-spill dispersal over five consecutive years (from 2016 to 2020) to provide robust monthly estimates of oil-spill risks. By combining them with marine traffic density, we can identify shipping pollution exposure hotspots corresponding to areas with high traffic density and high probability for an oil spill to reach a QVCI.

Results

Understanding the vulnerability of Qatar's desalination plants and LNG exporting facilities pertains to performing a quantitative assessment of the risk of oil spills, shipping pollution exposure and the arrival time of the latter as detailed in the following.

Oil-spill risk

Oil-spill risk spatial distribution maps highlight the offshore areas posing the greatest threat to QVCIs (Fig. 2a,b). Oil released in those areas has a high probability of being driven by currents to land on the shore of a given QVCI. Risk distributions exhibit a clear seasonality related directly to changes in the oceanic and atmospheric circulations. In the summer, the oceanic circulation in the Gulf is dominated by a large cyclonic (anticlockwise) gyre, and the atmospheric circulation is dominated by summer shamal winds[20]. Both lead to a strong southeastward circulation that results in risk patterns that extend in the northwest direction. Ras Laffan's risk pattern is the largest as it is located north of Qatar and hence not sheltered from the incoming southeastward circulation. The LNG terminal entry, being located about 7 km from the shore, is more exposed to oil spills than the intake of Ras Laffan desalination plant. Abu Fontas and Umm Al Houl are located farther south and are thus more sheltered from the southeastward circulation by Qatar mainland. They are therefore subject to a limited oil-spill risk (Fig. 2a). Similar, although weaker, circulation patterns are observed during winter months, leading to similar risk patterns. In spring and autumn, the oceanic circulation is more variable, with more mesoscale eddy activity[21]. The atmospheric circulation is also weaker and less directional[22,23]. As a result, the risk pattern of Ras Laffan is no longer unidirectional, and it now extends southwestwards. Abu Fontas and Umm al Houl have a broader risk pattern that extends farther east (Fig. 2b).

We estimate the monthly total risk (Fig. 2c) to which each QVCI is exposed by spatially integrating their respective monthly risk spatial distribution and normalizing it with respect to the largest monthly value for all four QVCIs (corresponding here to the LNG terminal of Ras Laffan in June; Fig. 1c). The LNG terminal of Ras Laffan is most at risk of being disrupted by an oil spill, with a total risk 4 to 5 times larger than for the desalination plants of Abu Fontas and Umm Al Houl. These southern QVCIs are more sheltered from currents by the embayed coastal morphology, especially during the summer and winter months. The seasonal risk evolution shows that Ras Laffan is out of phase with Abu Fontas and Umm al Houl, with the former being most at risk in winter and summer, while the latter two see their risks peak in spring and autumn.

Shipping pollution exposure

We then combine the monthly risk patterns (Fig. 2) with the annual marine traffic density (Fig. 1) to derive the exposure of QVCI to marine shipping oil pollution (Fig. 3a). This indicator assumes that the probability of accidental or intentional offshore oil discharge is proportional to the marine traffic density. The exposure patterns are therefore composed of hotspots corresponding to both high traffic density and high probability for an oil spill to reach a given QVCI. The locations of these exposure hotspots are unchanged throughout the year as they correspond to high-density regular shipping routes and vary only in their intensities. They can be clearly identified on a yearly averaged shipping pollution exposure map (Fig. 3a), where exposure values have been normalized with respect to the largest value. The areas with the largest exposure (>1% of maximum value; Fig. 3a) are concentrated in the immediate proximity of the ports of Ras Laffan and Doha, as well as along the route to the industrial area south of Mesaieed (see location on Fig. 1). These areas are within 10–15 km of the coast and close to marine surveillance authorities as Qatar's largest coast guard base is located halfway between Doha and Ras Laffan. Further away, the areas around the shipping routes to Bahrain and between Qatar and Iran also carry an important exposure (between 0.1 and >1%; Fig. 3a). The route to Bahrain's exposure is located mostly out of Qatar Exclusive Economic Zone (EEZ). Overall, Ras Laffan is exposed to oil pollution occurring in a rectangular area of about 120 km long and 30 km wide (~3,600 km^2 with >0.01% exposure; Fig. 3a), while Abu Fontas and Umm al Houl are exposed to oil pollution within a triangular area about 40 km wide and 60 km high (~1,200 km^2 with >0.01% exposure; Fig. 3a). There appears to be almost no oil pollution exposure associated with nearby oil and gas (O&G) fields such as Abu Safah in the Kingdom of Saudi Arabia (KSA) and North Field, Bul Hanine and Maydan Mahzam, all in Qatar.

We estimate the total shipping pollution exposure by integrating the monthly exposure spatial distributions of each QVCI and normalizing them by their largest value for all four QVCIs. The LNG terminal of Ras Laffan is markedly exposed to oil spills throughout the year, with little seasonal variability. Comparatively, the nearby desalination plant exhibits a more variable exposure profile (Fig. 3b), with high exposure in spring and autumn and a much lower exposure in winter and summer. This is due to the stronger southeastward atmospheric and oceanic circulation during those months that have a smaller impact on the desalination plant as it is more sheltered by the coastal topography than is the entrance of the LNG terminal. For Umm Al Houl and Abu Fontas desalination plants, the total exposures all year long are lower and exhibit the same seasonality as the total oil-spill risk, with slightly higher values in spring and autumn than during summer and winter due to the changes in the circulation patterns.

Oil-spill arrival time

Arrival-time patterns (Fig. 4a,b) represent the minimum time required by oil released in a 1 km grid element to reach the nearest QVCI. They indirectly represent the coupled atmospheric and oceanic circulation patterns. In early summer, when southeastward shamal winds are the strongest, the arrival-time pattern is skewed to the northwest, which means that an oil spill originating from Bahrain EEZ could reach Ras Laffan in two to three days (Fig. 4b). In spring and autumn, the more variable and turbulent circulation patterns could allow oil spills from the United Arab Emirates EEZ to reach Abu Fontas and Umm al Houl in less than two days (Fig. 4a). Among the shipping pollution exposure hotspots identified in Fig. 3a, the shipping routes to Bahrain and to Iran could pose a threat to Ras Laffan in two to four days (Fig. 4c), with the shortest arrival times observed in June. The desalination stations of Umm al Houl and Abu Fontas are threatened mostly by the routes between Doha and the industrial area south of Mesaieed. Since this route is close to the coast, the arrival time remains relatively stable throughout the year at about two days.

https://doi.org/10.1038/s41893-022-01037-w

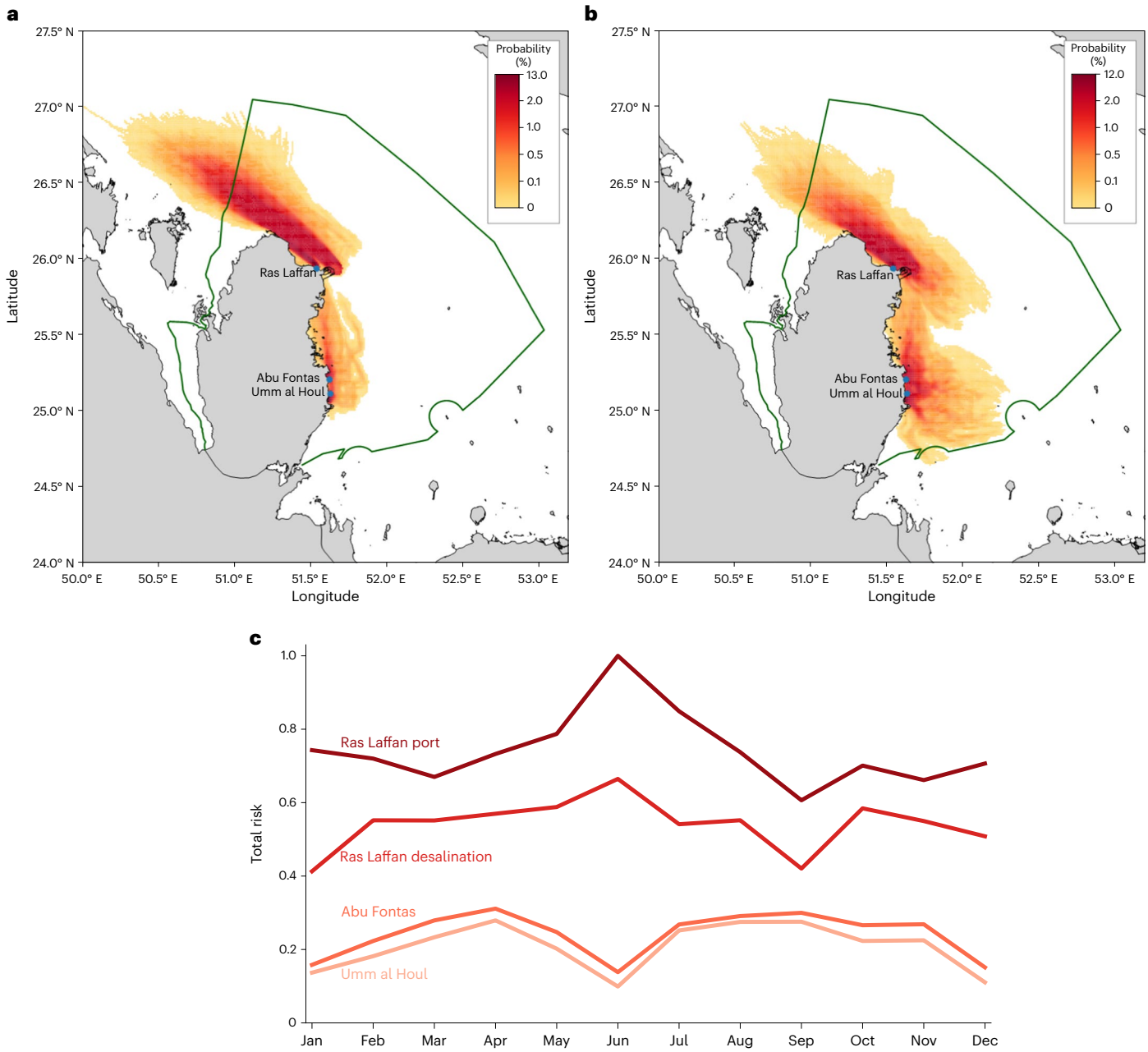

Fig. 2 | Spatial and temporal distributions of oil-spill risk. Oil-spill risk is defined as the probability of a coastal infrastructure being impacted by an oil spill. **a**,**b**, The spatial risk distributions for the months of June (**a**) and September (**b**) show that changes in the atmospheric and oceanic circulation patterns drive the orientation and extent of the risk patterns for the desalination and LNG export facilities. **c**, The monthly evolution of the total risk, defined as the spatial integral of the risk pattern of each coastal infrastructure and normalized by the largest monthly value, shows that June is the month carrying the most risk for the LNG terminal and desalination plant of Ras Laffan, while the two other desalination plants are mostly sheltered during that month. Oil-spill risks for Abu Fontas and Umm al Houl are the largest in spring and autumn, when the oceanic and atmospheric circulations are more variable.

Discussion

Qatar's LNG export and desalination facilities are all vulnerable to oil spills. Their risk patterns are driven directly by the atmospheric and oceanic circulations, which have a well-defined seasonality. In summer and winter, southeastward shamal winds can produce strong and directional circulation patterns that weaken in spring and autumn as they are replaced by a more variable and turbulent circulation. As a result, Ras Laffan LNG terminal and desalination plants are most at risk in summer and winter as they are located north of Qatar and hence exposed to the southeastward circulation. In summer and winter, the desalination plants of Abu Fontas and Umm al Houl are sheltered by the mainland. In spring and autumn, as the circulation becomes more variable, the risk patterns tend to shift east, hence increasing the risk for Abu Fontas and Umm al Houl and slightly reducing it for Ras Laffan (Fig. 2). When combining these risk patterns with marine shipping density, taken as a proxy to oil discharge probability, we can identify five major exposure hotspots: near the ports of Ras Laffan and Doha and along the routes to Mesaieed, Bahrain and Iran (Fig. 3). The first three are very close to the coastal QVCIs and hence probably closely monitored. The remaining two are located farther away and even outside of Qatar EEZ, in areas potentially less monitored by maritime surveillance authorities.

https://doi.org/10.1038/s41893-022-01037-w

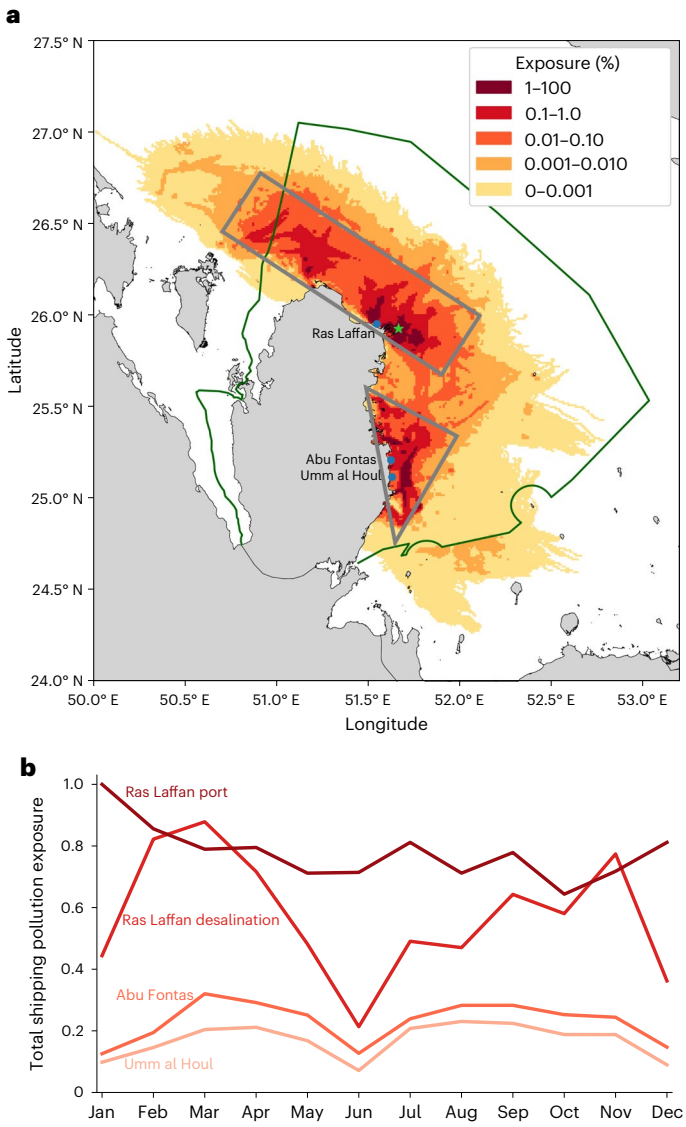

Fig. 3 | Spatial and temporal distributions of shipping pollution exposure. **a**, The yearly averaged shipping pollution exposure map highlights offshore locations with both high shipping traffic density and a high probability for an oil spill released there to reach a coastal infrastructure. The two areas where most of the shipping exposure is concentrated, covering about 4,800 km^2, are highlighted in grey. **b**, The monthly evolution of total shipping pollution exposure, defined as the spatial integral of the monthly exposure pattern of each coastal infrastructure and normalized by the largest monthly value, shows that the LNG terminal of Ras Laffan is the most exposed infrastructure. It is exposed to oil spills originating from marine traffic in its immediate vicinity as well as along the shipping routes to Iran and Bahrain. The shipping route to Bahrain is mostly outside of Qatar EEZ.

We have identified two offshore areas where most of the shipping oil pollution exposure is concentrated. They cover about 5,000 km^2, which is about 15% of Qatar's EEZ total area, but also extends out of it into Bahrain's coastal waters. The total size of those two areas can be entirely covered using one or two orbital SAR scenes, depending on the acquisition geometry. A combination of multiple SAR platforms in X and C bands for the defined areas can allow daily monitoring with a manageable data volume and reliable change detection to identify oil spills. Alternatively, airborne SAR can be deployed in these areas during high-vulnerability times to increase the frequency of the monitoring if or when needed. The increase in the acquisition frequency of SAR images in future Earth observation missions such as NiSAR for the Gulf area will be crucial to provide reliable early measurements. The most important risk area is the one associated with the industrial city of Ras Laffan, whose LNG terminal exports more than 20% of the globally consumed LNG and whose desalination plant produces more than 30% of Qatar's drinking water. Ras Laffan's offshore risk area is about 120 km long and 30 km wide, accounting for ~60% of the total vulnerability zone. Furthermore, it overlaps several major maritime routes where some of the world's largest oil tankers, LNG carriers and cargo vessels operate. Any major oil discharge along the shipping routes to Iran and Bahrain could impact the operation of the desalination and LNG export facilities of Ras Laffan in two to three days. The maritime activity along the route from Al Ruwais in Qatar to Iran was particularly intense during the blockade of Qatar enforced by neighbouring Gulf countries from mid-2017 to the beginning of 2021. Our results suggest that the future reproduction of such regional geopolitical instability could have indirect rippling effects on the global energy market as it increases Qatar's vulnerability to oil spills within Ras Laffan's exposure area.

Although our study is based on well-established models and data, it has limitations in portraying the complete picture associated with the occurrence of oil spills and their consequences. For example, we cannot assess the duration of port closure and desalination disruption as this depends on the nature and severity of the spill. Desalination plants are the most vulnerable as even a minor spill can clog the screens and filters and, for plants relying on reverse osmosis technology, damage the membrane[24]. In addition to these physical damages, the oil contains chemicals such as benzene, which are human carcinogens. The maximum permissible level of benzene in drinking water in the United States is set to five parts per billion[25]. The continued operation of desalination plants with even a small amount of benzene in the seawater could therefore pose a threat to public health. These elements suggest that, in the event of an offshore oil spill potentially threatening a desalination plant, stringent oil mitigation measures would be put in place (such as the installation of booms, fishnets and air-releasing hoses and the application of oil/water separation measures) to prevent the oil from reaching the plant intake. In the event of a major spill, the plant would probably be closed preemptively[12]. The proximity of Ras Laffan's LNG terminal to the desalination plant means that oil mitigation measures could also impede the navigation of LNG tankers and hence lead to port closure or severe maritime traffic disruption. The access in and out of the LNG export facilities could also be compromised without the latter being directly hit by the oil spill in the case where the pollution blocks one of the dredged canals that connect the facility to deeper navigable waters.

Our study highlights Qatar's combined water–energy vulnerability. Its main desalination and LNG export facilities are at risk of being disrupted by oil spills originating from a 5,000 km^2 offshore area. There are several factors that would make an oil spill in this identified area one with severe consequences at the regional and global scales. First, an important part of the exposure area occurs outside of Qatar EEZ, requiring international coordination and simulation exercises with Bahrain and Iran to increase the readiness for any major oil spill. Such international coordination is compromised by the tense political context among the three nations[6] and the fact that the last major regional oil-spill collaborative mitigations were four decades ago, following the Hasbah-6 well blowout in Saudi Arabia (1980) and from the Nowruz oil field (1983)[26]. Although Qatar could call for help through the Marine Emergency Mutual Aid Centre in Bahrain, as part of the Regional Organization for the Protection of the Marine Environment, and although it gained substantial experience during the mitigation efforts carried in these two events, the fact they occurred far back in time questions the country's current readiness to address such oil spills following years of tense diplomatic relations with its neighbouring Gulf countries. Second is the complexity of the bathymetry of the offshore vulnerability area where the seawater is mostly below 5–10 m depth.

https://doi.org/10.1038/s41893-022-01037-w

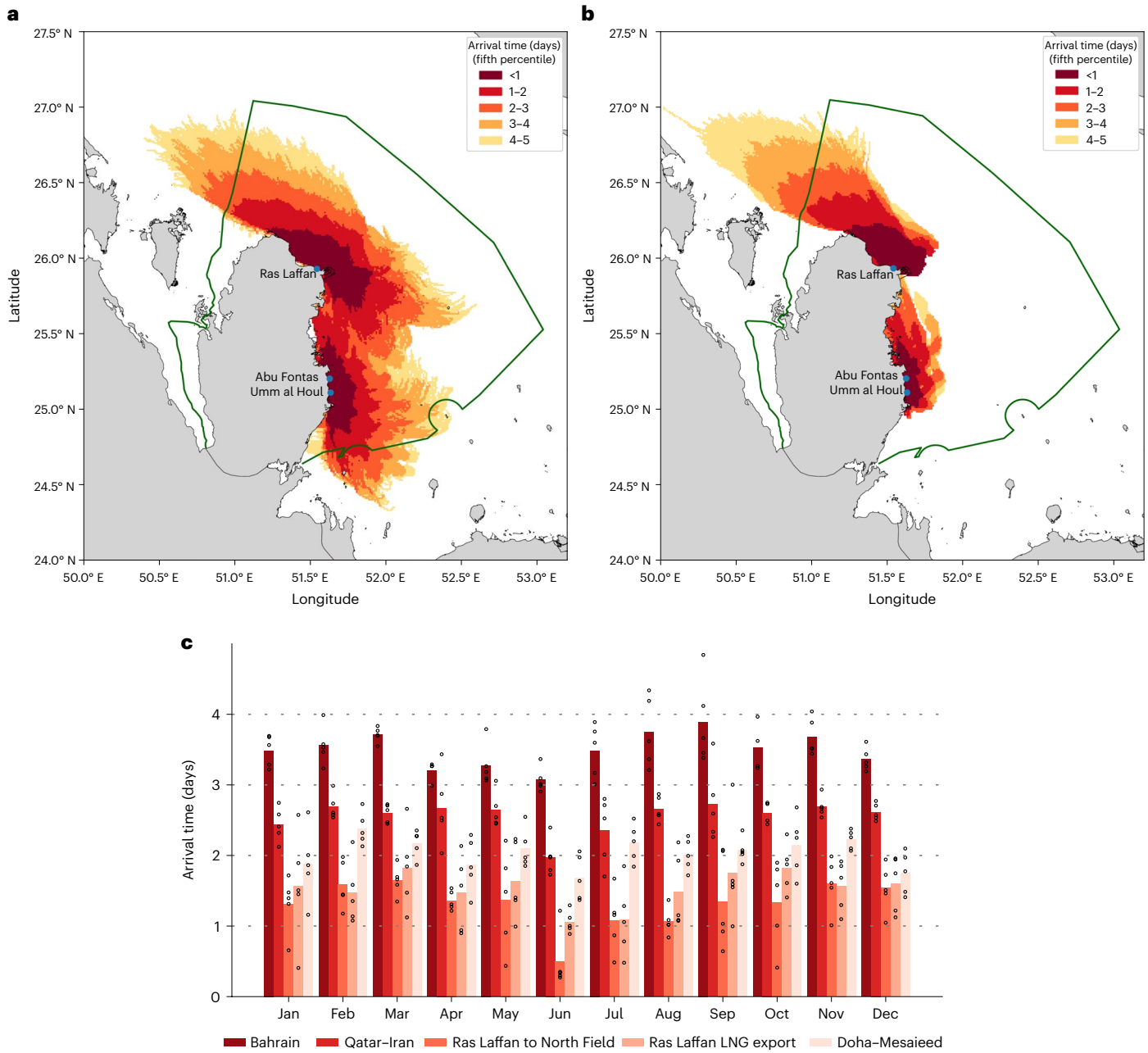

Fig. 4 | Spatial and temporal distributions of oil-spill arrival times. a,**b**, The arrival-time spatial distributions for the months of April (**a**) and June (**b**) show that Ras Laffan's infrastructure could be impacted in two to three days by oil spills originating from Bahrain's EEZ. In spring/autumn, the more variable atmospheric and oceanic circulations shift the arrival-time distributions to the east, hence allowing oil spills released in the United Arab Emirates' EEZ to reach Umm al Houl and Abu Fontas in less than two days. **c**, The monthly evolution for the mean arrival time to the nearest coastal infrastructure (averaged over the $n = 5$ simulated years shown by dots) for oil spills released along the main shipping routes shows that June is the most dangerous month, with minimal time to mitigate an oil spill.

The latter means that the arrival time to the coastline is overestimated if we account for the spill arrival into the shallow waters below 2 m where most large oil-spill mitigation vessels cannot operate in response to a major spill. Qatar's current contingency plan prescribes containment and recovery within 26 hours as the preferred response technique[27], with provision for the use of dispersants. But in such shallow waters, dispersants can be used only in far offshore areas. Hence, the arrival time of spills must be adjusted to a virtual coastline that is few kilometres away from the physical coast, reducing further the available time for mitigation. Third, the timing of peak vulnerability during the hot and dust-erosive summertime causes an additional challenge for mitigating large oil spills. Most containment plans rely on international contractors that may not be technically ready to operate under such harsh conditions under short notice in the summertime when also a large part of the expatriate labour force, representing more than 92% of the nation's workforce, could be out of the country and hence not able to support a fast containment.

In the event of a major oil spill threatening Ras Laffan, oil mitigation measures such as the deployment of booms to prevent the spill from reaching the coastline and the desalination plant intake would probably stop the traffic of LNG tankers. As the LNG market is expected to remain very tense over 2022–2026[28], such disruption would put

considerable pressure on global gas prices. In 2021, the cost of natural gas in Europe was an average of US$16 per metric million British thermal units (mmBtu), up from US$3 mmBtu^{-1} in 2020. It reached US$70 mmBtu^{-1} in August 2022[29]. While such an increase had negative consequences for European consumers and industries, it was worse in some Asian developing countries such as Pakistan and Bangladesh, whose electricity production relies on LNG bought on the spot market (at a price not determined by long-term pre-negotiated contracts with producers). Those countries could no longer afford to buy LNG at current prices, which led to power cuts that in turn fuelled social and political turmoil[30,31]. As energy prices keep rising, social unrest is now expected in European countries as well[32]. Any disruption to Ras Laffan's exports will thus be immediately felt and on a large scale that is yet to be quantified. For example, on Monday, 5 September 2022, gas prices in Europe surged by 30% after Russia shut the gas flow off completely through the Nord Stream 1 pipeline[33]. At the time of the shutdown, Nord Stream 1 was operating at just 20% of its capacity, hence exporting gas at a rate of about 10 b.c.m. yr^{-1}, which is less than a tenth of Qatar's exports from Ras Laffan.

A major oil spill could therefore trigger two crises that Qatari authorities would have to manage simultaneously: disrupted LNG exports and water scarcity. Qatar currently has water reserves slightly above two days, and it is planning to extend them to seven days by 2026[34] under average usage conditions. It is important to note that Qatar has a clear seasonal variability in its water usage, with the highest consumption occurring during the winter season due to the larger expatriate population being present in the country during work months and the recent agricultural developments. Therefore, if only one desalination plant had to be shut down, the country could run into severe water shortage in less than a week. Such water shortage problems would further complicate oil-spill mitigation due to the panic effect that can be caused among the large expatriate population, which is mostly exogenic to the desert environment and could be unfamiliar with water scarcity mitigation measures. It is hence important to note that for the upcoming four years, until the deployment of the large strategic water reserve systems that will store 2,300 million gallons in 24 individual reservoirs, the nation's vulnerability to oil spills will be alarming. Globally, any minor disruption to the natural gas supply would send tremors through the world economy. As of today, the natural gas market has minimal spare capacity and is thus very sensitive to such potential disruption. Prices in regions with limited production and storage capacity, such as Europe and Asia, have reached their highest levels in years[35]. Any disruption to the Ras Laffan terminal, which exports more than 20% of LNG consumed globally, would have dire consequences.

Methods

Oil-spill model

We simulate oil-spill dispersal with OpenOil, which is part of the OpenDrift trajectory modelling library developed at the Norwegian Meteorological Institute (MET Norway)[36]. OpenOil is an open-source full-fledged three-dimensional oil-spill model that shares many similarities with other commercial software and open-source codes such as SIMAP, OSCAR, OILMAP, MOHID and MEDSLIK-II. OpenOil is used operationally by MET Norway[37] and has been thoroughly validated against satellite and airborne observations of oil slicks in the North Sea[38]. It has been used in a number of oil vulnerability assessments such as in the Aegean Sea[39] and in the Straits of Florida[40].

Like most oil-spill models, OpenOil is a Lagrangian model that represents an oil spill as an ensemble of oil particles. These particles are transported horizontally by the three-dimensional ocean currents, the surface wind-generated waves through the so-called Stokes drift, which is equal to 1.5% of the wind velocity at the surface and decreases with depth[41], and the wind that yields an additional surface velocity equal to 2% of the wind velocity. Since the Stokes drift and the ocean currents' velocity change with depth, it is important to represent the oil particles' vertical dynamics. This depends on several factors. First, oil particles at the surface can be entrained below the ocean surface by breaking waves, which is parameterized in OpenOil with the algorithm of Li et al.[42]. Second, the vertical dynamics are also influenced by oil-particle buoyancy, which is calculated from the empirical relationship of ref. [43]. It depends on the oil viscosity, oil density, seawater temperature, salinity and oil droplet size distribution. The droplet size distribution is calculated with the algorithm of ref. [44]. Within the water column, oil particles are subject to vertical turbulence, which is based on the turbulent eddy diffusivity parameterization of ref. [45]. Finally, oil weathering processes are included in OpenOil by using the evaporation, emulsification and dispersion parameterizations included in ADIOS OilLibrary, the National Oceanic and Atmospheric Administration library of oils and their properties[46].

Oil-spill transport simulations can be conducted forwards and backwards in time. The forward approach amounts to simulating the future evolution of a spill movement from its release point up to its destination. It yields an estimation of the area that will be impacted by an oil spill released at a certain location and at a given time. The forward approach is typically used for operational forecasting and contingency planning[47]. This modelling approach has also been used in several vulnerability assessments, including in the Gulf[48], where the source of oil is known (for example, offshore wells, busy shipping lines or O&G terminals) and the coastal area impacted by the spill is unknown. The backward approach amounts to simulating the past evolution of the spill by starting from its final position and going backwards in time to estimate where the spill originated[49]. That approach is the most efficient when the impacted area is known but the geographical source of pollution is undefined. It has already been used in the Mediterranean Sea[50] and in the Arabian Sea[51] but, to our knowledge, never in the Gulf. Backward simulations retain a stochastic dynamic to represent the uncertainty on the particles' position due to unresolved subgrid-scale processes. This uncertainty increases as the particles move backwards in time[49]. Here we represented it by taking a horizontal diffusivity of 2 m^2 s^{-1}. We chose that value as it corresponds or is similar to the default horizontal diffusivity values used in the GNOME[52] and MEDSLIK-II[53] oil-spill models.

For the backward simulation approach, oil weathering processes, which lead to changes in the oil chemical composition and physical characteristics, cannot be considered as they are not time-reversible processes. The type of oil has therefore a limited impact on the results of a backward simulation as it influences only the vertical dynamics of the oil particles through their specific droplet size distribution, density and viscosity. While the oil-spill mass balance cannot be directly computed by the model, it could be estimated by using empirical relations that express the mass of oil left in the spill in terms of the time elapsed since the oil release, the type of oil and water temperature[54].

The duration of each backward simulation is set to five days. This rather limited duration is due to two factors. First, in five days the spill can generally travel a distance larger than the distance from Qatar's coastline to the limit of its EEZ. This means that Qatar's local authorities would not be able to directly use the information provided by longer simulations to deploy mitigation measures as they would have to be placed outside of their territorial waters. Second, the horizontal diffusivity leads to a spreading of the spill that increases like $(K_h \times t)^{1/2}$, where $K_h = 2$ m^2 s^{-1}. After five days, the uncertainty on the spill location is about 930 m, which is close to the resolution of the grid used to compute the risk indicators. This is also compounded by the uncertainty on the modelled wind and ocean currents driving the spill dynamics. There is thus a trade-off between the duration of the backward simulations and the resolution of the risk indicators. If the simulation duration increases, then the accuracy of the risk indicators decreases. We have therefore selected a five-day duration as a good trade-off between the accuracy and usability of our results. The same duration has further been used in other oil vulnerability assessments based on backward simulations[50].

Since the objective of this study is to estimate the vulnerability of Qatar desalination and LNG export facilities to oil spills, the backward approach is the best suited. We considered Qatar Marine oil, a medium oil with a specific gravity of 32.65° API. Qatar Marine oil is the most common type of hydrocarbon extracted from the oilfields close to Qatar. However, it is not the only type of oil present in the Gulf and transported by oil tankers. The type of oil used in the simulation has a limited impact on the backward oil-spill modelling results as it influences only the vertical oil distribution and not the oil weathering processes. We performed a sensitivity analysis with other types of oils (for example, IFO-180LS, a heavy oil of 15.9° API that is used as fuel for shipping) and found very similar results. To initiate the backward simulations, oil particles are released from receptor points located on a 2-km-radius circle around the desalination plant intake and the LNG terminal entry. A total of about 100 particles are released from each QVCI on every day of the 2016–2020 period at midnight. The transport of a total of ~7×10^5 particles is then simulated during the five-year period. Particles reaching the coastline during their backward displacement can no longer be re-entrained in the water column. Such stranded particles indicate the location of potential onshore sources of pollution that are not considered in this study as we focus on offshore sources.

Table 1 | Vessel types with the largest cumulative dry weight tonnage that navigated in the Gulf during 2019

Vessel type	Mean age (yr)	% Occurrence	% Total DWT
Crude oil tanker[a]	11.0	6.4	52.7
Bulk carrier	12.1	4.9	12.0
Container ship	13.8	5.0	10.4
Tanker[a]	9.4	0.9	5.0
LNG tanker[a]	12.5	1.2	4.3
Oil/chemical tanker[a]	11.3	3.6	4.2
Oil products tanker[a]	16.3	2.1	3.0
LPG tanker[a]	11.7	1.3	1.8
Floating storage/production[a]	20.4	0.1	1.2
Self-discharging bulk carrier	5.6	0.1	0.3
Cabu carrier	9.3	0.0	0.1

More than 50% of the total dry weight tonnage (DWT) transported in 2019, considered herein as the reference year for unperturbed maritime transport, was carried by crude oil tankers, which made up 6.4% of all vessels navigating the Gulf. [a]Vessels carrying O&G products.

Metocean data

The oil-spill dynamic is driven by the combined effect of ocean currents, wind and waves over the 2016–2020 period. For the ocean currents, we used the outputs of the global ocean circulation model NEMO (Nucleus for European Modelling of the Ocean[55]). The physical ocean component of NEMO solves the three-dimensional ocean circulation primitive equations for the velocity field, sea surface elevation, temperature and salinity. It uses a global curvilinear orthogonal grid in the horizontal direction and a mixture of *z* and *s* coordinates in the vertical direction. NEMO model outputs are distributed by Mercator Ocean, the French centre for analysis and forecasting of the global ocean. Mercator Ocean operates global forecasting systems and produces global and regional reanalysis, all based on NEMO ocean model, coupled with a data assimilation system. For this study, we used the outputs of the global forecasting system that include daily mean sea level, temperature, salinity and currents, as well as hourly mean surface fields. The global ocean output files are displayed with a 1/12° horizontal resolution and 50 vertical levels ranging from 0 to 5,500 metres. Since the 1/12° grid of the ocean model NEMO does not entirely cover the nearshore area, we extended that grid by one or two grid elements and extrapolated model variables on the new grid points. Oil particles are therefore subject to realistic non-zero ocean currents everywhere in the domain. The wind velocity data are retrieved from the European Centre for Medium-Range Weather Forecasts (ECMWF) Reanalysis v.5 (ERA5). They have a spatial resolution of 30 km and a temporal resolution of one hour. The wave data are retrieved from the global third-generation MFWAM wave model. It runs on a 1/12° grid and provides three-hourly instantaneous outputs. Model outputs are also distributed by Mercator Ocean. Supplementary Video 1 shows the time evolution of the oceanic and atmospheric circulation patterns in the central part of the Gulf during the entire year 2020.

Using the outputs of the global atmosphere and ocean models to drive the oil spills' dynamics does not allow us to represent all the complexity of the circulation patterns. For example, ERA5 wind data do not include land and sea breezes, which are known to locally influence wind patterns in the Gulf[56]. In the ocean, NEMO's 1/12° horizontal resolution cannot represent eddies and flow features occurring at a scale smaller than about 10 km. The ocean model resolution is, however, fine enough to represent the main mesoscale eddies that have a typical size of about 110–130 km and the baroclinic Rossby deformation radius of about 25–30 km (ref. [21]). OpenOil has already been used with NEMO and ERA5 outputs. It is equipped with the interpolating functions needed to compute the value of the ocean and wind velocities at the positions of the oil particles[36]. OpenOil is run with a five-minute time step, hence much smaller than the daily and hourly time steps of the ocean and atmosphere model outputs.

Marine traffic data

We derived a marine traffic density map from the automatic identification system used by all vessels larger than 300 tons to report their position (Fig. 1). The automatic identification system data have been purchased from MarineTraffic, a community-based project that provides information on ship movements[57], for the entire year 2019. As this was the last full year before the COVID19 pandemic, we assumed that marine traffic during that year was representative of normal shipping activity in the Gulf. MarineTraffic data show that Qatar is surrounded by a very dense network of shipping routes that connect the O&G fields, ports and industrial terminals throughout the Gulf (Fig. 1). Within Qatar's EEZ, an offshore area of about 31,590 km^2 under Qatar's sovereignty, the busiest routes connect Al Ruwais to Iran, the port of Ras Laffan to the O&G platforms in Qatar's North Field, the port of Ras Laffan to the main shipping routes crossing the Gulf, and Doha to the industrial area South of Mesaieed. The route to Khalifa Bin Salman Port (Manama, Bahrain) also passes through Qatar EEZ and becomes denser as it approaches the port. The traffic density map further highlights the locations of major O&G fields such as Abu Safah (KSA), North Field, Bul Hanine and Maydan Mahzam (Qatar). The MarineTraffic data also include information on vessel type, age, tonnage and flag. In 2019, 72.3% of the transported mass across the Gulf consisted of O&G products that were carried by 15.7% of all vessels (Table 1). Moreover, most of these vessels were registered outside of the Gulf area (Extended Data Table 1), where safety, operational and accountability requirements are often less stringent than the local rules.

Risk indicators

The backward oil-dispersal simulations produced an ensemble of trajectories starting from the receptor points around each QVCI and moving backwards in time. By meshing the sea surface with a 1 km grid, we can compute the number of trajectories that intersect each grid element during each month of the 2016–2020 period, as well as the travel time for the oil spill to move from the receptor points to the grid element. By dividing the number of trajectories that cross each grid element during a given month by the total number of trajectories that originated from the receptor points during that time, we obtain a probability map. It indicates, for each grid element, the probability for

that grid element to be a source of pollution that will reach the receptor point during that month. It can also be interpreted as the fraction of all the oil released in that element during the month that would reach the receptor point[50].

Oil-spill risk (Fig. 2a,b) is formally defined as the combination of the probability of being impacted by a spill and its consequences[58]. We assume that these consequences are comparable for all four QVCI. The risk indicator, therefore, corresponds with the probability for an oil spill released within a 1 km grid element during a given month to reach a QVCI. Monthly risk distribution maps have been averaged over the 2016–2020 period to account for the interannual variability of the atmospheric and oceanic circulations in the Gulf.

A time-of-arrival map (Fig. 4) is computed by taking the minimum time needed for oil released in a grid element to reach the receptor point. Herein, we define this minimum time as the 5% quantile of the arrival-time distribution, corresponding to the time such that 95% of all cases have values larger than this duration. Both the probability and arrival-time maps were computed for every month of the 2016–2020 period (a total of 60 months). We then took the average over the five years for each month of the year to obtain statistically reliable monthly estimates.

The exposure of QVCI to oil pollution originating from marine traffic is assumed to be directly proportional to marine traffic density; that is, the more vessels navigating in a certain area, the higher the probability of accidental or intentional oil release in that area. In this study, we consider both minor and major oil spills. The former typically involve less than 50 barrels (corresponding to about 7 tons) of oil released[59] and are, for example, occurring during operational discharges. Major oil spills, involving the release of hundreds to thousands of barrels, are the result of major accidents, such as collisions or grounding, and are much less frequent. Even if minor spills might not directly restrict large vessels' navigation, the oil-spill containment measures that would be deployed to prevent the spill from reaching the coastline would impede navigation, hence indirectly leading to port closures.

We derive the shipping pollution exposure indicator by multiplying the oil pollution probability with the marine traffic density, which indicates the number of shipping routes that crossed each grid element. Our approach is similar to that of Quattrocchi et al.[60], who also assume that the probability of oil spills is proportional to maritime traffic density. While they consider a forward-in-time modelling approach and hence estimate the probability for a coastal segment to be hit by a spill, they estimate this probability like in our study and then combine it with maritime traffic density to obtain an indicator similar to the exposure one used here.

Reporting summary

Further information on research design is available in the Nature Portfolio Reporting Summary linked to this article.

Data availability

The oil-dispersal simulation outputs for every month and every coastal infrastructure are available at https://zenodo.org/record/7340698 (https://doi.org/10.5281/zenodo.7340697). The atmospheric and oceanic circulation data used to force the oil-dispersal model are freely available at https://www.ecmwf.int/en/forecasts/datasets/reanalysis-datasets/era5 and https://data.marine.copernicus.eu/products. The marine traffic data used to compute the shipping exposure indicator can be purchased at https://www.marinetraffic.com/en/p/ais-historical-data.

Code availability

The oil-spill dispersal simulations were performed with the open-source model OpenOil (version 1.60) available at https://opendrift.github.io. The Python programmes used to produce the key results of this study are available at https://forge.uclouvain.be/dobbelaeret/scripts_anselain2022_natsustain.

References

1. *GIIGNL 2021 Annual Report* (GIIGNL, 2021); https://giignl.org/publications/giignl-2021-annual-report
2. Hofste, R. W., Reig, P. & Schleifer, L. *17 Countries, Home to One-Quarter of the World's Population, Face Extremely High Water Stress* (World Resources Institute, 2019)
3. Abotalib, A. Z., Heggy, E., Scabbia, G. & Mazzoni, A. Groundwater dynamics in fossil fractured carbonate aquifers in Eastern Arabian Peninsula: a preliminary investigation. *J. Hydrol.* **571**, 460–470 (2019).
4. Mohieldeen, Y. E., Elobaid, E. A. & Abdalla, R. GIS-based framework for artificial aquifer recharge to secure sustainable strategic water reserves in Qatar arid environment peninsula. *Sci. Rep.* **11**, 18184 (2021).
5. Darwish, M. A. & Mohtar, R. Qatar water challenges. *Desalination Water Treat.* **51**, 75–86 (2013).
6. Hussein, H. & Lambert, L. A rentier state under blockade: Qatar's water–energy–food predicament from energy abundance and food insecurity to a silent water crisis. *Water* **12**, 1051 (2020).
7. *Water Sector* (Kahramaa, accessed 30 August 2022); https://www.km.qa/Aboutus/Pages/Watersector.aspx
8. *Annual Statistics Report 2020* (Kahramaa, 2021); https://www.km.qa/MediaCenter/Publications/Annual%20Statistics%20Report%202020%20English.pdf (2021)
9. Dale, S. *bp Statistical Review of World Energy 2021* (bp, 2022); https://www.bp.com/content/dam/bp/business-sites/en/global/corporate/pdfs/energy-economics/statistical-review/bp-stats-review-2022-full-report.pdf
10. El Gamal, R. Qatar Petroleum signs deal for mega-LNG expansion. *Reuters* (8 February 2021).
11. *Global Gas Outlook to 2050* (McKinsey & Company, 2021); https://www.mckinsey.com/~/media/mckinsey/industries/oil%20and%20gas/our%20insights/global%20gas%20outlook%20to%202050/global-gas-outlook-2050-executive-summary.pdf
12. Surkes, S. 2017 oil spill closed three desalination plants for three days, official reveals. *The Times of Israel* (19 March 2021).
13. Aizhu, C. & Blanchard, B. China seals oil port after spill. *Reuters* (19 July 2010).
14. Huynh, B. Q. et al. Public health impacts of an imminent Red Sea oil spill. *Nat. Sustain.* https://doi.org/10.1038/s41893-021-00774-8 (2021).
15. *Annual Statistical Bulletin* (OPEC, 2021); https://asb.opec.org
16. Evtushenko, N., Ivanov, A. & Evtushenko, V. in *Advances in Remote Sensing and Geo Informatics Applications* (eds El-Askary, H. M. et al.) 343–347 (Springer, 2019).
17. Sheppard, C. et al. The Gulf: a young sea in decline. *Mar. Pollut. Bull.* **60**, 13–38 (2010).
18. *Worldwide Rig Counts—Current & Historical Data* (Baker Hughes, 2021); https://rigcount.bakerhughes.com/intl-rig-count
19. Garcia-Pineda, O. et al. Classification of oil spill by thicknesses using multiple remote sensors. *Remote Sens. Environ.* **236**, 111421 (2020).
20. Al Azhar, M., Temimi, M., Zhao, J. & Ghedira, H. Modeling of circulation in the Arabian Gulf and the Sea of Oman: skill assessment and seasonal thermohaline structure. *J. Geophys. Res. Oceans* **121**, 1700–1720 (2016).
21. Thoppil, P. G. & Hogan, P. J. A modeling study of circulation and eddies in the Persian Gulf. *J. Phys. Oceanogr.* **40**, 2122–2134 (2010).
22. Thoppil, P. G. & Hogan, P. J. Persian Gulf response to a wintertime shamal wind event. *Deep Sea Res. 1* **57**, 946–955 (2010).
23. Yu, Y., Notaro, M., Kalashnikova, O. V. & Garay, M. J. Climatology of summer shamal wind in the Middle East: summer shamal climatology. *J. Geophys. Res. Atmos.* **121**, 289–305 (2016).

24. Tahir, F., Baloch, A. A. B. & Ali, H. in *Sustainability Perspectives: Science, Policy and Practice: A Global View of Theories, Policies and Practice in Sustainable Development* (eds Khaiter, P. A. & Erechtchoukova, M. G.) 303–329 (Springer, 2020); https://doi.org/10.1007/978-3-030-19550-2_15
25. *Benzene* (ATSDR, 2015); https://www.atsdr.cdc.gov/sites/toxzine/docs/benzene_toxzine.pdf
26. Al-Amirah, A. S. The Nowruz oil spill in the Arabian Gulf: case study of Saudi Arabia. *Geogr. Bull.* **37**, 16–32 (1985).
27. Marhoon, Y. *Qatar Response Plan* Version 5 (OSRL, 2021); https://www.oilspillresponse.com/globalassets/external-links/covid-19-updates/emea---qatar-response-090420-1030.pdf
28. *Global LNG Market Outlook 2022–26* (Bloomberg, 2022); https://bbgmktg.turtl.co/story/global-lng-market-outlook/
29. *Commodity Markets* (World Bank, accessed 23 August 2022); https://www.worldbank.org/en/research/commodity-markets
30. Stapczynski, S. Global energy crunch is making gas too pricey for Asia. *Bloomberg* (17 June 2022).
31. Yep, E. Factbox: Asia-Pacific economies face escalating energy crisis. *S&P Global Commodity Insights* (27 June 2022).
32. Gill, J. Analysis: heat or eat? Winter protests loom as energy poverty sweeps Europe. *Reuters* (25 August 2022).
33. Twidale, S. & Buli, N. EU gas price rockets higher after Russia halts Nord Stream flows. *Reuters* (5 September 2022).
34. *Water Security Mega Reservoirs Project* (Kahramaa, accessed 11 October 2021); http://www.watermegareservoirs.qa
35. Natural-gas prices are spiking around the world. *The Economist* (21 September 2021).
36. Dagestad, K.-F., Röhrs, J., Breivik, Ø. & Ådlandsvik, B. OpenDrift v1.0: a generic framework for trajectory modeling. *Geosci. Model Dev.* **11**, 1405–1420 (2018) https://doi.org/10.5194/gmd-11-1405-2018
37. Barker, C. H. et al. Progress in operational modeling in support of oil spill response. *J. Mar. Sci. Eng.* **8**, 668 (2020).
38. Röhrs, J. et al. The effect of vertical mixing on the horizontal drift of oil spills. *Ocean Sci.* **14**, 1581–1601 (2018).
39. Keramea, P., Kokkos, N., Gikas, G. & Sylaios, G. Operational modeling of North Aegean oil spills forced by real-time met–ocean forecasts. *J. Mar. Sci. Eng.* **10**, 411 (2022).
40. Androulidakis, Y., Kourafalou, V., Robert Hole, L., Le Hénaff, M. & Kang, H. Pathways of oil spills from potential Cuban offshore exploration: influence of ocean circulation. *J. Mar. Sci. Eng.* **8**, 535 (2020).
41. Breivik, Ø., Bidlot, J.-R. & Janssen, P. A. E. M. A Stokes drift approximation based on the Phillips spectrum. *Ocean Model.* **100**, 49–56 (2016).
42. Li, Z., Spaulding, M. L. & French-McCay, D. An algorithm for modeling entrainment and naturally and chemically dispersed oil droplet size distribution under surface breaking wave conditions. *Mar. Pollut. Bull.* **119**, 145–152 (2017).
43. Tkalich, P. & Chan, E. S. Vertical mixing of oil droplets by breaking waves. *Mar. Pollut. Bull.* **44**, 1219–1229 (2002).
44. Li, Z., Spaulding, M., French McCay, D., Crowley, D. & Payne, J. R. Development of a unified oil droplet size distribution model with application to surface breaking waves and subsea blowout releases considering dispersant effects. *Mar. Pollut. Bull.* **114**, 247–257 (2017).
45. Sundby, S. A one-dimensional model for the vertical distribution of pelagic fish eggs in the mixed layer. *Deep Sea Res. A* **30**, 645–661 (1983).
46. Lehr, W., Jones, R., Evans, M., Simecek-Beatty, D. & Overstreet, R. Revisions of the ADIOS oil spill model. *Environ. Model. Softw.* **17**, 189–197 (2002).
47. Zodiatis, G. et al. The Mediterranean Decision Support System for Marine Safety dedicated to oil slicks predictions. *Deep Sea Res. 2* **133**, 4–20 (2016).
48. Amir-Heidari, P. & Raie, M. Probabilistic risk assessment of oil spill from offshore oil wells in Persian Gulf. *Mar. Pollut. Bull.* **136**, 291–299 (2018).
49. Batchelder, H. P. Forward-in-time-/backward-in-time-trajectory (FITT/BITT) modeling of particles and organisms in the coastal ocean. *J. Atmos. Ocean. Technol.* **23**, 727–741 (2006).
50. Ciappa, A. C. Reverse trajectory study of oil spill risk in Cyclades Islands of the Aegean Sea. *Reg. Stud. Mar. Sci.* **41**, 101580 (2021).
51. Suneel, V., Ciappa, A. & Vethamony, P. Backtrack modeling to locate the origin of tar balls depositing along the west coast of India. *Sci. Total Environ.* **569–570**, 31–39 (2016).
52. Zelenke, B., O'Connor, C. & Barker, C. *General NOAA Operational Modeling Environment (GNOME) Technical Documentation* (NOAA OR&R, October 2012); https://response.restoration.noaa.gov/gnome_manual
53. De Dominicis, M., Pinardi, N., Zodiatis, G. & Archetti, R. MEDSLIK-II, a Lagrangian marine surface oil spill model for short-term forecasting—part 2: numerical simulations and validations. *Geosci. Model Dev.* **6**, 1871–1888 (2013).
54. Fingas, M. in *Oil Spill Science and Technology* (ed. Fingas, M.) 243–273 (Elsevier, 2011); https://doi.org/10.1016/B978-1-85617-943-0.10010-3
55. Madec, G. NEMO ocean engine. *Zenodo* (2017) https://doi.org/10.5281/zenodo.3248739
56. Eager, R. E. et al. A climatological study of the sea and land breezes in the Arabian Gulf region. *J. Geophys. Res.* **113**, D15106 (2008).
57. MarineTraffic: Global Ship Tracking Intelligence (accessed 15 May 2021) https://www.marinetraffic.com/
58. Etkin, D. S. et al. in *Oil Spill Science and Technology* 2nd edn (ed. Fingas, M.) 71–183 (Gulf Professional Publishing, 2017); https://doi.org/10.1016/B978-0-12-809413-6.00002-3
59. *Oil Tanker Spill Statistics 2021* (ITOPF, 2022); https://www.itopf.org/knowledge-resources/data-statistics/statistics/
60. Quattrocchi, G. et al. An operational numerical system for oil stranding risk assessment in a high-density vessel traffic area. *Front. Mar. Sci.* **8**, 585396 (2021).

Acknowledgements

The authors thank J. Lawler and M. Vermeersch from Qatar Environment and Energy Research Institute for the helpful discussion on the country's oil-spill mitigation plan and B. Shomar from Qatar University for the discussion on water reserves in Qatar. Computational resources were provided by the Consortium des Équipements de Calcul Intensif (CÉCI), funded by the F.R.S.-FNRS under grant no. 2.5020.11. E. Heggy acknowledges support from the Zumberge Research and Innovation Fund of the University of Southern California (USC) allocated to the Arid Climates and Water Research Center—AWARE. Part of E. Heggy's research was carried out at USC under contract from the Jet Propulsion Laboratory, California Institute of Technology, under a contract with the National Aeronautics and Space Administration (NASA) (OASIS-SAA-00630). The funders had no role in the study design, data collection and analysis, decision to publish or preparation of the manuscript.

Author contributions

E. Hanert and E. Heggy designed the experiment. T.A. and T.D. conducted simulations. All the authors examined the results and wrote the manuscript.

Competing interests

The authors declare no competing interests.

Additional information

Extended data is available for this paper at https://doi.org/10.1038/s41893-022-01037-w.

Supplementary information The online version contains supplementary material available at https://doi.org/10.1038/s41893-022-01037-w.

Correspondence and requests for materials should be addressed to Essam Heggy or Emmanuel Hanert.

Peer review information *Nature Sustainability* thanks Johannes Röhrs, Simonetta Cheli, and the other, anonymous, reviewer(s) for their contribution to the peer review of this work.

https://doi.org/10.1038/s41893-022-01037-w

Extended Data Table 1 | Flag distribution for the vessels that navigated in the Gulf during 2019, considered herein as the reference year for unperturbed maritime transport

Vessel flag	% Occurrence
Panama	18,1%
Liberia	14,4%
Marshall Is	12,1%
Singapore	5,8%
Hong Kong	5,3%
Malta	4,5%
Iran	4,3%
Bahamas	3,1%
India	2,7%
Greece	2,6%
Cyprus	2,0%

Vessels are ranked in terms of their total dry weight tonnage, and we show only vessel flags accounting for at least 2% of all occurrences.

nature research

Corresponding author(s): Emmanuel Hanert

Last updated by author(s): Nov 21, 2022

Reporting Summary

Nature Research wishes to improve the reproducibility of the work that we publish. This form provides structure for consistency and transparency in reporting. For further information on Nature Research policies, see our Editorial Policies and the Editorial Policy Checklist.

Statistics

For all statistical analyses, confirm that the following items are present in the figure legend, table legend, main text, or Methods section.

n/a	Confirmed	
☐	☒	The exact sample size (*n*) for each experimental group/condition, given as a discrete number and unit of measurement
☒	☐	A statement on whether measurements were taken from distinct samples or whether the same sample was measured repeatedly
☒	☐	The statistical test(s) used AND whether they are one- or two-sided *Only common tests should be described solely by name; describe more complex techniques in the Methods section.*
☒	☐	A description of all covariates tested
☒	☐	A description of any assumptions or corrections, such as tests of normality and adjustment for multiple comparisons
☐	☒	A full description of the statistical parameters including central tendency (e.g. means) or other basic estimates (e.g. regression coefficient) AND variation (e.g. standard deviation) or associated estimates of uncertainty (e.g. confidence intervals)
☒	☐	For null hypothesis testing, the test statistic (e.g. *F*, *t*, *r*) with confidence intervals, effect sizes, degrees of freedom and *P* value noted *Give P values as exact values whenever suitable.*
☒	☐	For Bayesian analysis, information on the choice of priors and Markov chain Monte Carlo settings
☒	☐	For hierarchical and complex designs, identification of the appropriate level for tests and full reporting of outcomes
☒	☐	Estimates of effect sizes (e.g. Cohen's *d*, Pearson's *r*), indicating how they were calculated

Our web collection on statistics for biologists contains articles on many of the points above.

Software and code

Policy information about availability of computer code

Data collection	No software was used to collect the data
Data analysis	Oil spill simulations were done using the open source model OpenOil (version 1.60) on Python (version 3.6.12). OpenOil includes the NOAA oil library ADIOS. All data analysis was conducted on Python (version 3.6.12). The Python programs used to produce the key results of this study are available at https://forge.uclouvain.be/dobbelaeret/scripts_anselain2022_natsustain.

For manuscripts utilizing custom algorithms or software that are central to the research but not yet described in published literature, software must be made available to editors and reviewers. We strongly encourage code deposition in a community repository (e.g. GitHub). See the Nature Research guidelines for submitting code & software for further information.

Data

Policy information about availability of data

All manuscripts must include a data availability statement. This statement should provide the following information, where applicable:

- Accession codes, unique identifiers, or web links for publicly available datasets
- A list of figures that have associated raw data
- A description of any restrictions on data availability

The oil dispersal simulation outputs for every month and every coastal infrastructure are available at https://zenodo.org/record/7340698 (doi: 10.5281/zenodo.7340697). The atmospheric and oceanic circulation data used to force the oil dispersal model are freely available at https://www.ecmwf.int/en/forecasts/datasets/reanalysis-datasets/era5 and https://data.marine.copernicus.eu/products. The marine traffic data used to compute the shipping exposure indicator can be purchased at https://www.marinetraffic.com/en/p/ais-historical-data.

Field-specific reporting

Please select the one below that is the best fit for your research. If you are not sure, read the appropriate sections before making your selection.

☐ Life sciences ☐ Behavioural & social sciences ☒ Ecological, evolutionary & environmental sciences

For a reference copy of the document with all sections, see nature.com/documents/nr-reporting-summary-flat.pdf

Ecological, evolutionary & environmental sciences study design

All studies must disclose on these points even when the disclosure is negative.

Study description	Evaluation of oil spill risk in the Arabian Gulf for Qatar's main LNG export and desalination facilities using an oil spill dispersal model forced with data-assimilated oceanic and atmospheric model outputs.
Research sample	This is unapplicable because our work is a simulation study. No samples or observational data were collected.
Sampling strategy	This is unapplicable because our work is a simulation study. No samples were collected.
Data collection	This is unapplicable because our work is a simulation study. No observational data were collected.
Timing and spatial scale	The oil spill dispersal simulations were run over five consecutive years (2016-2020) in order to account for the interannual variability in the oceanic and atmospheric circulation.
Data exclusions	No data was excluded
Reproducibility	Experiment can be repeated following the methods described. The oil spill dispersal model is open source. The oil dispersal model outputs are available at https://zenodo.org/record/7340698. The oil dispersal model forcings can be freely downloaded from ECMWF and CMEMS.
Randomization	This is unapplicable because our work is a simulation study and our study design does not incorporate experimental groups
Blinding	This is unapplicable because our work is a simulation study and our study design does not incorporate experimental groups

Did the study involve field work? ☐ Yes ☒ No

Reporting for specific materials, systems and methods

We require information from authors about some types of materials, experimental systems and methods used in many studies. Here, indicate whether each material, system or method listed is relevant to your study. If you are not sure if a list item applies to your research, read the appropriate section before selecting a response.

Materials & experimental systems

n/a	Involved in the study
☒	☐ Antibodies
☒	☐ Eukaryotic cell lines
☒	☐ Palaeontology and archaeology
☒	☐ Animals and other organisms
☒	☐ Human research participants
☒	☐ Clinical data
☒	☐ Dual use research of concern

Methods

n/a	Involved in the study
☒	☐ ChIP-seq
☒	☐ Flow cytometry
☒	☐ MRI-based neuroimaging